CHAPTER 6

Photonic Bandgap Glass-Based Structures

M. Clara Gonçalves[1] and Amadeu Griol[2]

[1]Departamento de Engenharia Química, Instituto Superior Técnico, Universidade de Lisboa, Portugal and [2]Valencia Nanophotonics Technology Center, Universitat Politècnica de València, Camí de Vera, s/n, 46022 València, Spain

Abstract: Photonic crystals (PCs) as it is often called photonic band gap materials (PBGs), are artificial composite materials, micro/nanostructured on an optical length scale (*e.g.* few hundreds of nm). The resulting periodicity in the dielectric constant is responsible for inhibiting light from propagating through the material as a result of Bragg diffraction. The forbidden frequency range is called a stop band. In PCs the electromagnetic waves within the band gap are completely reflected by the crystal, while spontaneous emission (within the band gap) are totally concealed.

This chapter introduces the physical concepts behind PC structures, along with bottom-up fabrication methods, properties, and applications.

1. INTRODUCTION

Gem opals, wings of butterflies and peacocks, fish scales, beetles, among a large number of other biological and mineral materials exhibit iridescence, strong multiple scattering, and unexpected forbidden wave propagation in certain frequency ranges (Fig. **1**). Nanostructured systems are in the basis of such behaviour [1, 2].

Photonic crystals (PCs) are the artificial counterparts. PCs as it is often called photonic band gap materials (PBGs) are artificial composite materials, micro/nanostructured on an optical length scale (*e.g.* few hundreds of nm). The resulting periodicity in the dielectric constant ε (or in the refractive index n, $n=\sqrt{\varepsilon}$) is responsible for inhibiting light (of frequencies in the visible or near infra-red range) from propagating through the material as a result of Bragg diffraction [3]. The forbidden frequency range is called a stop band. In PCs the electromagnetic waves within the band gap are completely reflected by the crystal, while spontaneous emission (within the band gap) are totally concealed.

***Corresponding author** ??? ?? ???

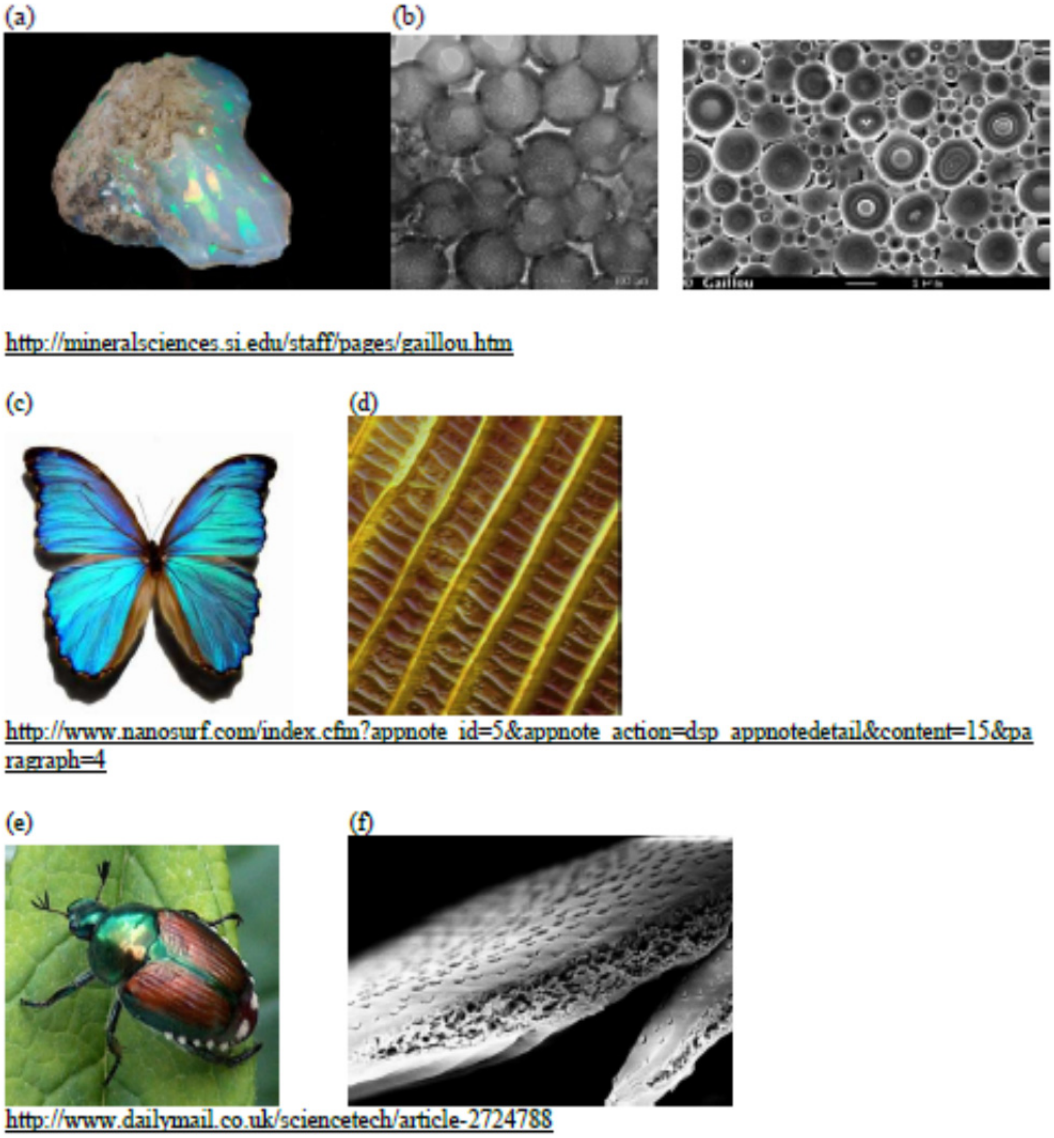

Figure 1: Biological and mineral iridescent materials and respective nanostructure: (a)-(b) gem opal, (c)-(d) wings of butterfly, (e)-(f) beetles.

PBGs can be in one, two or three dimensions (1D, 2D or 3D) (Fig. **2**), function of the dimensionality of the refractive index periodicity. A complete PBG, where all electromagnetic propagation is disallowed whatever the direction of propagation or the polarization, is only possible in 3D structures. Further, the dielectric constants ratio of the composite materials must be higger than 2.8.

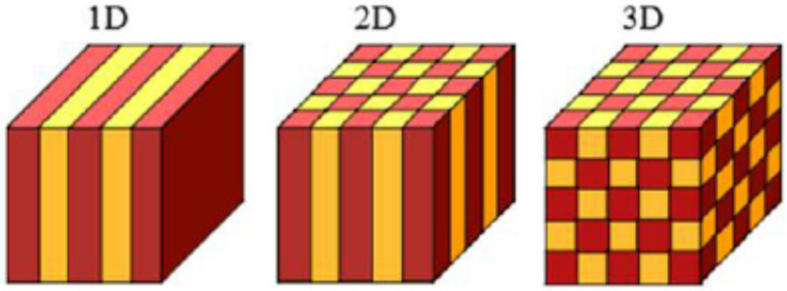

Figure 2: Schematics of 1D, 2D and 3D PCs. Distinct colors stand for different dielectric materials [3].

PCs are the optical analogue of electronic bandgap in semiconductors; it is believed that PCs should be able to transfer the full functionality of semiconductor devices into the all optical field, combining high integration with high speed processing.

PCs have attracted much interest due to the innumerous technological applications resulting from the multiple ways in which PCs may control and customize the flow of light, as the inhibition of spontaneous emission processes, the existence of photonic bandgaps (PBGs), or the confinement of light at defects. Besides they promise a large number of applications in different scientific and commercial areas like novel types of waveguides and optical fibers, new filters, high-speed switches, low-threshold microlasers, high-performance LEDs (light emitting diode), photonic for VLSI (very large scale integration), along with novel biological and chemical sensors (see 7. Photonic Crystals Applications).

Traditionally, both top-down and bottom-up approaches have been used to fabricate PCs. The methodology chosen often depends on the dimensionality of the PCs under studied-2D, for example, are often fabricated through gas source molecular beam epitaxy, two-photon lithography, direct-write electron-beam lithography, reactive-ion etching, oxidation processes or holographic methods, all top-down methodologies. 1D and 3D structures are often fabricated through bottom-up sol-gel protocols [2-7 and references wherein]. All these methods are based and take profit of current nanotechnology processes and fabrication system capable of operating and patterning at the sub wave scale. Fig. **3** shows SEM (scanning electron microscope) pictures of 1D and 2D PCs fabricated on SOI (silicon-on-insulator) technology, by combining electron beam lithography and etching processes; Fig. **4** illustrates SEM micrographs of 3D PCs fabricated by sol-gel methodology.

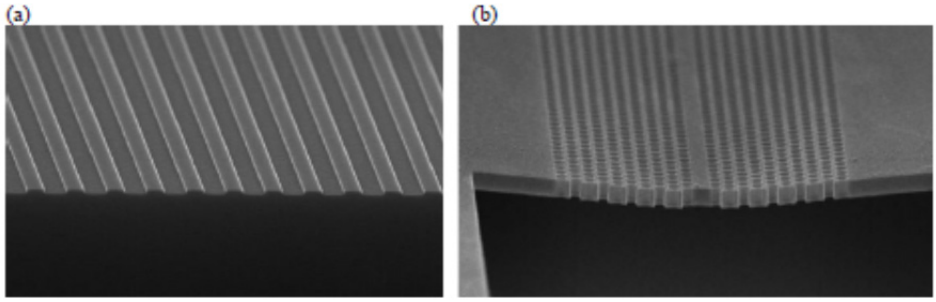

Figure 3: SEM pictures of: (a) 1D and (b) 2D PCs in SOI technology fabricated by electron beam lithography.

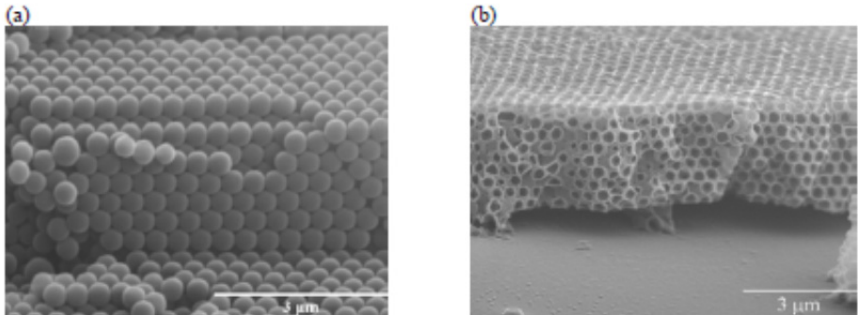

Figure 4: SEM micrographs of 3D PCs fabricated by sol-gel technology: (a) opal and (b) inverted opal.

2. PHOTONIC CRYSTALS-PHYSICAL PRINCIPLES

To understand the physical principles behind PCs, it is helpful to start with their electronic analogues. As excellently explained in ref. [3], a crystal can be defined as a periodic arrangement of molecules or atoms repeated in space according to a crystal lattice. The constituents of the crystal (patterns: atoms, ions, molecules) as well as its geometric lattice (and there are 14 Bravais lattices) define the crystal structure which rules the conduction properties of the crystal, *i.e.*, the way electrons will propagate through the crystal periodic potential. Electrons propagate as waves, and waves that meet certain criteria can travel through a periodic potential without scattering. But, in addition, the periodic lattice may inhibit the propagation of some waves, creating gaps in the crystal energy band where electrons are inhibited to propagate in specific directions. Moreover, if the lattice potential is sufficiently strong, a complete band gap, covering all possible propagation directions could be reached. This is what happens, for example, in semiconductor materials where a complete band gap between the valence and conduction energy bands is observed.

In a PC, the periodic dielectric constant (or refraction index) will replace the periodic potential. So, when the dielectric constants of the distinct composite materials differ adequately and their light absorption is minimal, then the PC can produce (with photons) many of the phenomena the semiconductor does with electrons. So, PC can provide a solution of light control and manipulation. Summarizing, PCs or PBG materials, are artificial dielectric nano-or micro-structured assemblies, where the refractive index modulation creates stop bands (EM) inside a certain frequency range, in 1D, 2D or 3D dimensions [3, 10].

In order to have a deeper knowledge about the electromagnetic behavior of PC, we recommend to the readers the PCs bible ref. [3]. Here we are going to introduce a brief and first approach.

Starting from the Maxwell equations and applying them to a mixed dielectric media as PCs suppose, we arrive to a linear Hermitian eigenvalue problem.

MAXWELL'S EQUATIONS

$$\begin{cases} \nabla \cdot \{\varepsilon(\vec{r})\vec{E}(\vec{r},t)\} = 0 \\ \nabla \cdot \vec{H}(\vec{r},t) = 0 \\ \nabla \times \vec{E}(\vec{r},t) = -\mu_0 \dfrac{\partial \vec{H}(\vec{r},t)}{\partial t} \\ \nabla \times \vec{H}(\vec{r},t) = \varepsilon_0 \varepsilon(\vec{r}) \dfrac{\partial \vec{E}(\vec{r},t)}{\partial t} \end{cases}$$

WAVE EQUATIONS

$$\nabla \times \left\{ \frac{1}{\varepsilon(\vec{r})} \nabla \times \vec{H}(\vec{r},t) \right\} = -\frac{1}{c^2} \frac{\partial^2 \vec{H}(\vec{r},t)}{\partial^2 t}$$

$$\frac{1}{\varepsilon(\vec{r})} \nabla \times \left\{ \nabla \times \vec{E}(\vec{r},t) \right\} = -\frac{1}{c^2} \frac{\partial^2 \vec{E}(\vec{r},t)}{\partial^2 t}$$

$$\vec{E} = \vec{E}(\vec{r}) \exp(-i\omega t)$$

$$\vec{H} = \vec{H}(\vec{r}) \exp(-i\omega t)$$

EIGENVALUE PROBLEM

$$L_E \vec{E}(\vec{r}) = \frac{\omega^2}{c^2} \vec{E}(\vec{r})$$

$$L_H \vec{H}(\vec{r}) = \frac{\omega^2}{c^2} \vec{H}(\vec{r})$$

With these equations (1-10), the dispersion diagrams (band diagrams) of different structures can be obtained. Fig. **5** shows an example of a 1D PC structure.

3. OPTICAL CHARACTERIZATION

There are a large number of techniques for the optical characterization of PCs structures. For the optical characterization of 1D and 3D systems, optical reflectance and transmission are the more common ones [12, 13]. In a reflectance setting-up, a high symmetry facet of the PC is chosen [14]. In a transmission setting-up, the detector is settled in alignment with the sample, alloying the

detection of the Bragg reflected photons. On the contrary, in specular reflectance setting-up, a Bragg plane is avoided as this experiment does not rely on detecting the scattered photon but its absence.

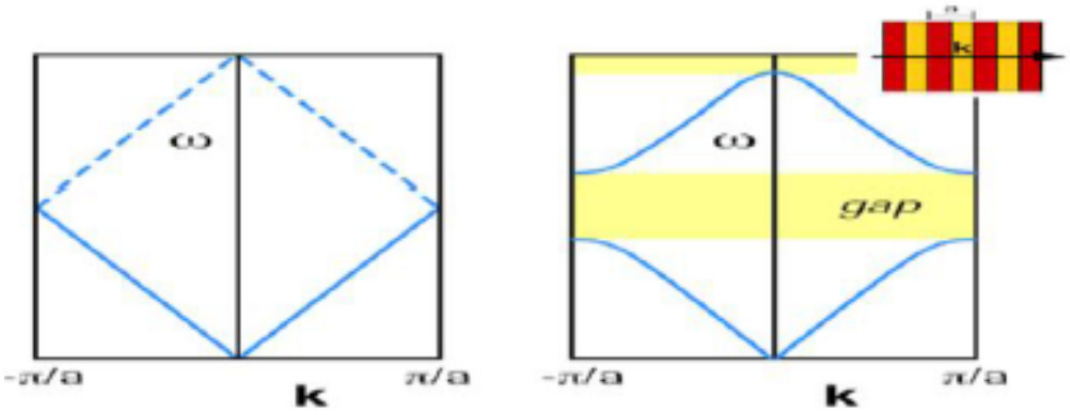

Figure 5: (a) Band diagram of a uniform 1D medium (dispersion relation: frequency, ω, *versus* wavenumber, k).(b) Schematic effect on the band diagram where a gap has been opened (adapted from [11]).

Now let's see what happens when light shines upon an artificial opal. Here certain wavelengths of the incident light do not penetrate very far the opal crystal but instead they are selectively reflected or scattered (from the periodic patterns, like the (111) plane in fcc structures) (Fig. **6**). In full PBG structure, each wavelength is reflected exactly at the same frequency as the incident light, regardless its direction or polarization state. Then, wherever the radiation interferes constructively, a colored crystal will be observed. Within the wavelength range where light is forbidden to propagate through the PC, a stop band will be recorded. The remaining transmitted light generates the complementary color.

By comparison with X-ray diffraction, the interaction of light (within the visible region) with the PC is described by the Bragg's law for the optical range, which considers Snell's law of refraction [16]:

$$\lambda = 2d\sqrt{n_{eff}^2 - \sin^2\theta} \tag{11}$$

where λ is the free space wavelength of the light, d the interplanar spacing between the scattering planes, θ is the angle between the incident radiation and the normal to the set of planes and n^2_{eff} is the effective dielectric constant of the composite PC (Fig. **6**). As the (111) plane has the highest planar density in the fcc

arrangement, with spacing $d_{hkl} = \frac{a}{\sqrt{h^2 + k^2 + l^2}}$ and $d_{(111)} = \frac{a}{\sqrt{3}}$, where $a = \frac{2D}{\sqrt{2}}$ and D is the sphere diameter in a colloidal PC, the longest wavelength diffracted by the *fcc crystal* will be:

$$\lambda_{\max} = 2n_{eff}\frac{D\sqrt{2}}{\sqrt{3}} = 1.633 n_{eff} D \qquad (12)$$

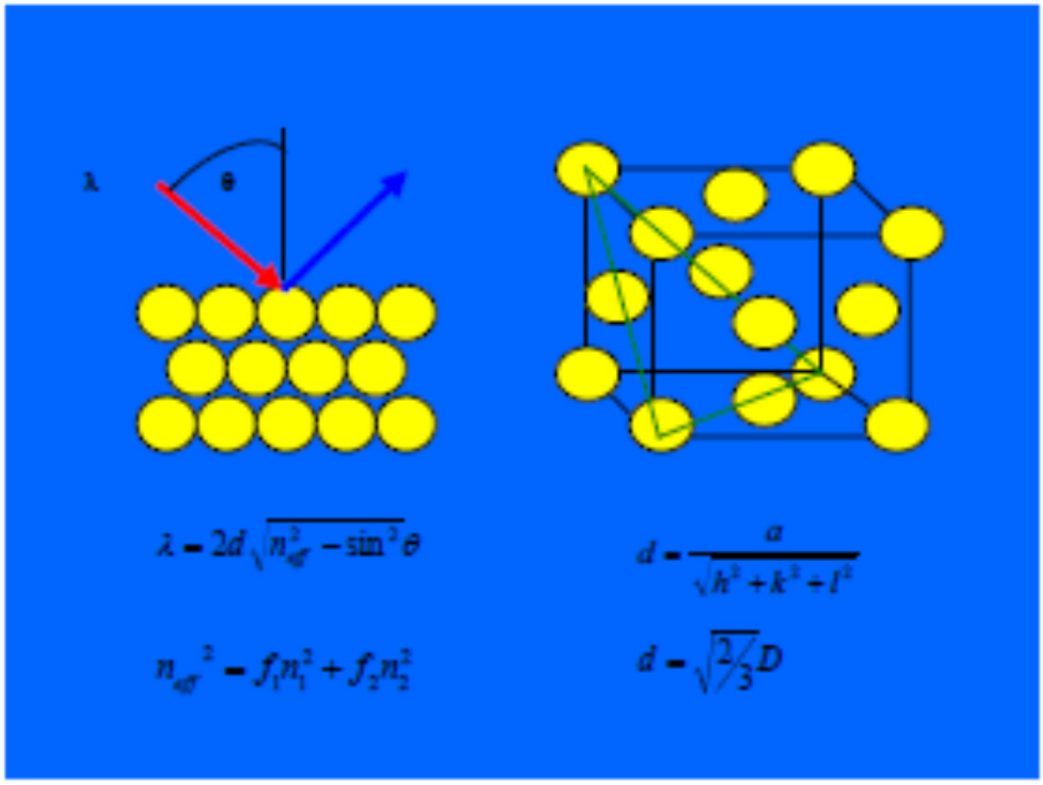

Figure 6: Diffraction of white light by fcc opals, at the (111) crystal planes. The highest density plane (111) exhibited a d(111) spacing, which is related to the sphere diameter, D. (Adapted from Ref. [15]).

When the sphere's diameter has the same magnitude as the visible light's wavelength, the artificial opal will act as a 3D diffraction lattice in the visible range where its color is established by the diameter of the spheres and the RI of the composite (Fig. **7**).

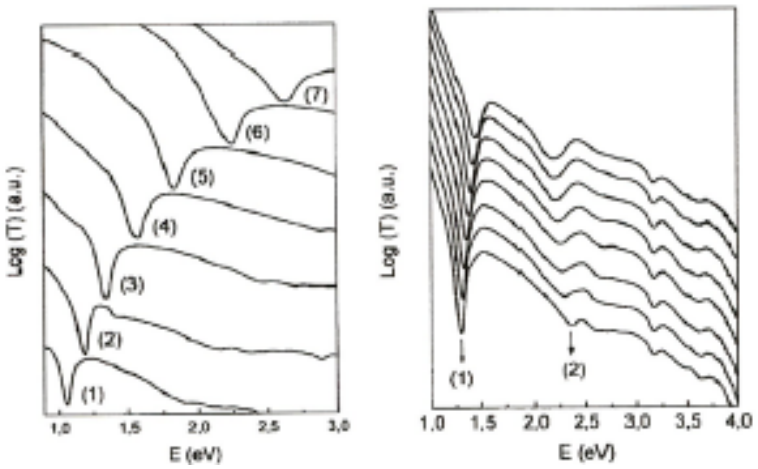

Figure 7: (a) Optical transmission at normal incidence (θ = 0º) for artificial opal structures, self-assembled of spheres with different diameters: (1) 535 nm, (2) 480 nm, (3) 415 nm, (4) 350 nm, (5) 305 nm, (6) 245 nm, and (7) 220 nm. (Reproduced with permission from ref. [17]).

On the other hands, 1D or 2D planar PC can be characterized by tunable laser and optical spectrometer at lab. This is the typical characterization method to carry out measures of light guiding where light is coupled directly to the waveguides (butt-coupling) or by means of grating couplers. A typical set-up for this kind of measurements is shown in Fig. **8**. The set-up includes polarization controllers, high resolution positioners, cameras and optical fibers.

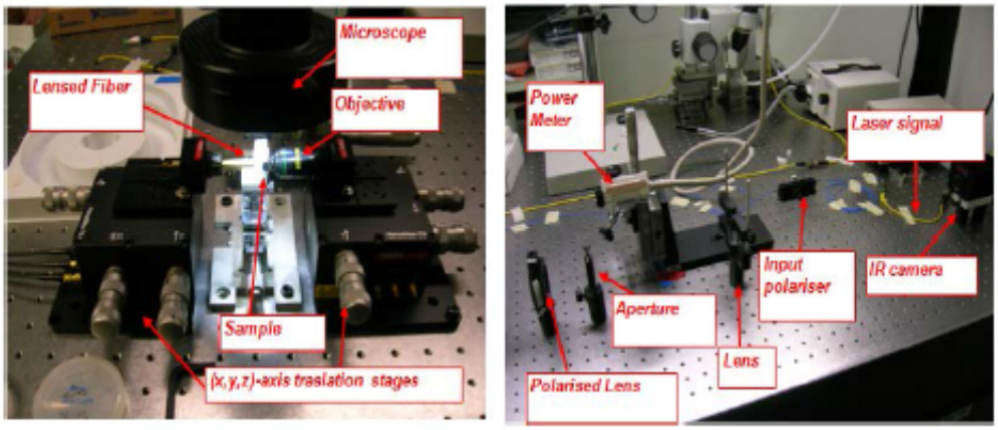

Figure 8: Measurement set-up for optical characterization of planar PC structures.

Fig. **9** depicts a typical optical response of a 2D PC fabricated on SOI technology which was characterized with the set-up shown in Fig. **8**.

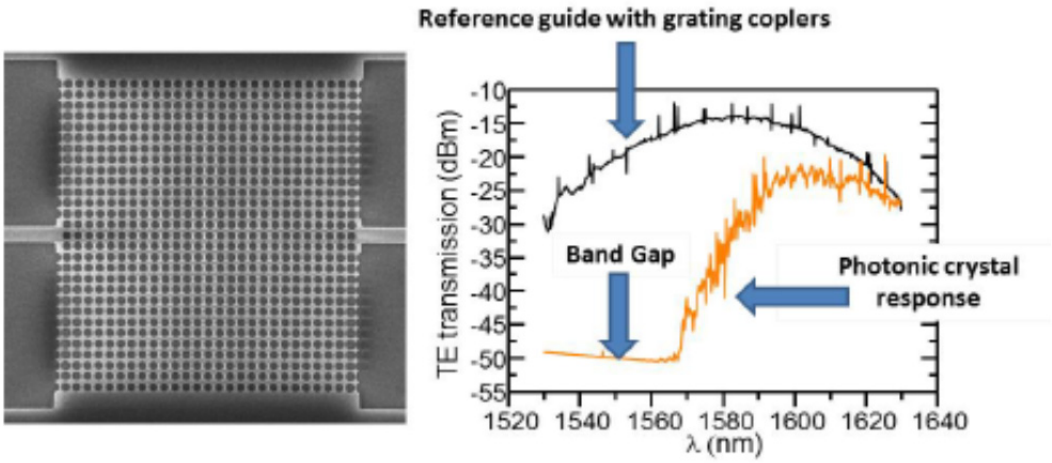

Figure 9: 2D photonic structure on SOI technology and its optical response.

Finally, other techniques for optical measurement of photonic have been used with high accuracy, as for example, those based on the use of tapered silica fiber loop to couple in and out light from the PC [18].

4. PHOTONIC CRYSTALS-FABRICATION METHODS AND RESULTING STRUCTURES

Gem opal is a natural iridescent material. In the gem opal, amorphous SiO2 spheres self-assemble into regular fcc globules, cemented by an amorphous silica matrix holding more SiO2 amorphous spheres [2]. The mimic of natural opal crystals is hence an interesting way to achieve PC's materials.

For near-IR frequencies, bottom-up techniques offer many potential advantages in 1D and 3D PCs fabrication. Competing top-down approaches, involving micromanipulation [19], lithography and selective etching techniques [20-23], or 3-D holography by means of multiple laser beams [24-28] exhibited considerable higher costs along with lower VLSI compatibility. In addition, bottom-up approaches offer an extraordinary versatility regarding to the materials used in fabricating PCs. The weak point appears to be the reduced crystalline area/volume of the fabricated material and the presence of huge number of random defects.

Among bottom-up approaches, the colloidal self-assembling method has been particularly studied. Colloidal techniques include electrostatically induced crystallization [29-33], gravity sedimentation [34-37], electro-hydrodynamic deposition[38-41], colloidal epitaxy [42], physical confinement [43, 44],

centrifugation [45], vertical convective self-assembly [46-51] and Langmuir-Blodgett films.

1D PCs Structures

Bragg mirrors, with a reflectivity (Bragg reflectivity) higher than that of metallic mirrors, are the most studied 1D PCs.

Bragg mirror structures consist of an assemblage of dielectric layers with alternating high and low refractive indices. The optical thickness, nx, of each layer equals is given by:

$$nx=\lambda/4 \quad (13)$$

λ being the wavelength of Bragg reflection, n the RI of the material and x the layer thickness.

The RI contrast and the number of layers are the project key parameters. The reflectivity of the stop-band increases with the RI contrast and the number of layers, being SiO2, TiO2 and ZrO2 the most common selected materials, due to the differences in their RIs.

Sol-gel Bragg mirrors are usually made by dip-[52-55] or spin-coating [6, 7, 56-59] techniques (see 3D PCs structures).

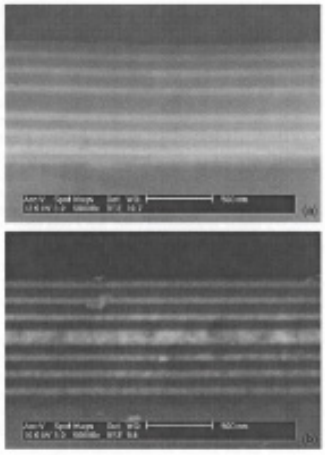

Figure 10: a) SEM cross-section image of a SiO2/TiO2 microcavity, forming by 12 alternating layers, and a silica defect layer; (b) SEM cross-section image of a SiO2/TiO2 microcavity, forming by 12 alternating layers, and a titania defect layer.

3D PCs structures

Vertical Convective Self-assembly

Vertical convective self-assembly deposition [46-49] is carry out with a substrate vertically positioned inside a bottle containing a colloidal suspension of monosized spheres (Figs. 11 and 12). As the solvent (and unreacted precursors) evaporate and the meniscus moves downwards the spheres of SiO2, TiO2, polystyrene (PS), poly(methyl methacrylate) (PMMA) *etc*., owing to their isotropic electrostatic potential, self-assemble into high atomic factor fcc or hc structures (Fig. **13**).

The optical Bragg reflections of artificial opal crystals deposited on the substrate appear as colored reflections to the unaided eye. By adjusting the colloidal concentration and the colloidal volume in the vial, the thickness of the deposit can be controlled. Notwithstanding, convective self-assembly produces small crystalline volume/area, demanding long processing times (within ~ 3-5 weeks).

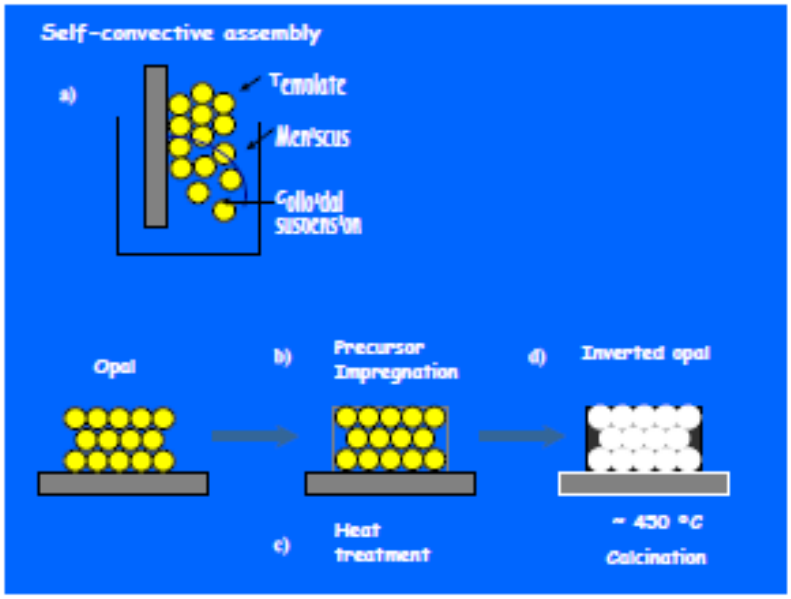

Figure 11: Fabrication of an artificial inverted opal by convective self-assembly: a) colloidal particles self-assemble into a fcc crystal on the surface of a substrate; b) once the template is formed, the interstices of the artificial opal are uniformly infiltrated with a higher RI material through a sol-gel process; c) a heat treatment is performed in order to achieve a solid structure from the sol-gel precursors; d) finally, the inverse-opal crystal (the negative of an opal structure) is attained through remotion of the original template material by heat treatment (for PS or PMMA), or etching in hydrofluoric acid (for silica colloids).

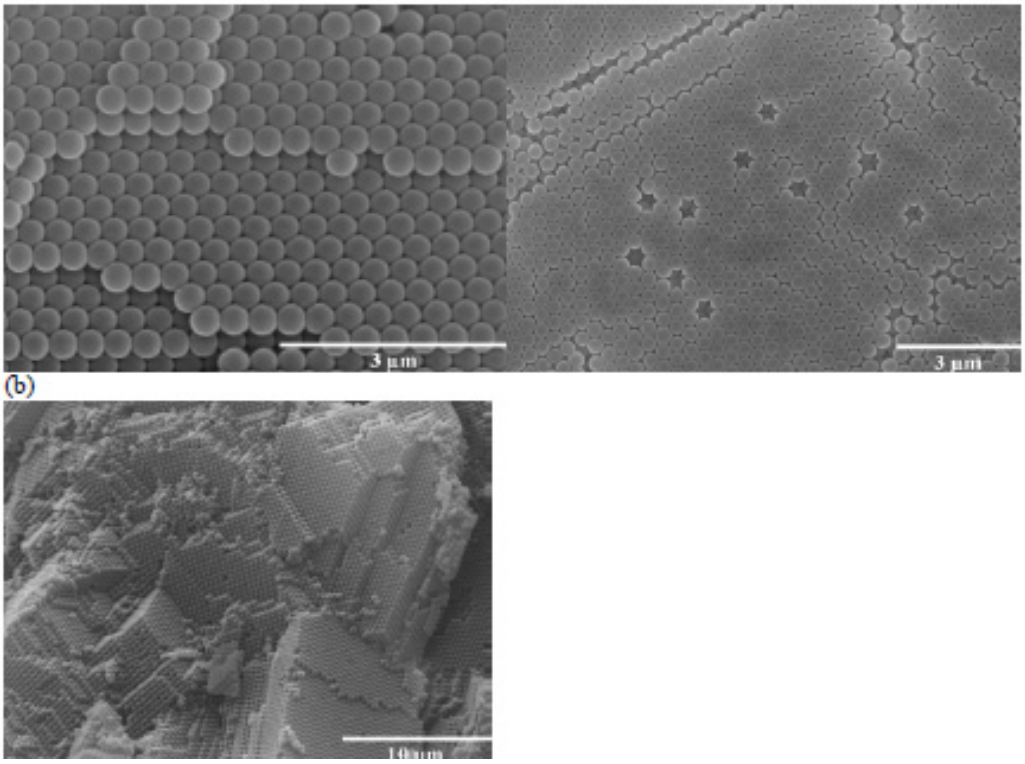

Figure 12: SEM micrograph of a typical opal made of 460 nm diameter PS spheres prepared by self-convective assembly: (a) top view; (b) cleaved edge showing different crystalline planes, {100} and {111}, of the fcc structure.

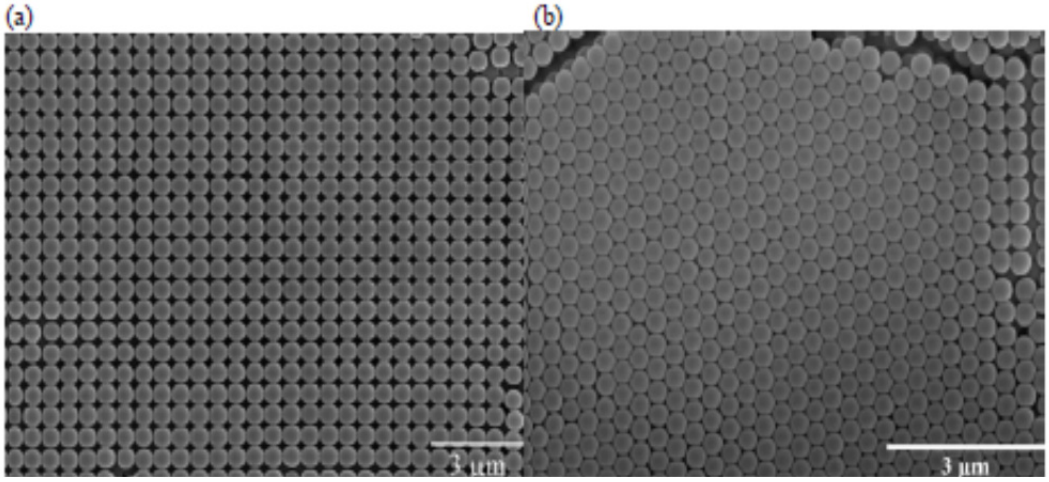

Figure 13: SEM micrograph of artificial opals: (a) hc structure and (b) fcc structure, prepared from self-convective assembled.

Artificial opals made of spheres of 150 nm in diameter, exhibited the suitable size for PCs operating in the optical range, but, insufficient RI contrast. Remember that to achieve a complete 3D PBG structures, the constituent materials' dielectric constants ratio must be larger than 2.8. So, the removal of the templates by chemical etching or calcination, followed by infiltration by a high RI dielectric material, followed by, will heighten the PBG behaviour of the composite nanostructure.

Semiconductor infilling may enhance the PBG properties, or inhibit the spontaneous emission of any emitting guest [60]. Careful choice of both the template sphere diameter and infiltrated semiconductor material allows the matching of the PC bandgap to the semiconductor emission.

Dip-Coating

Dip-coating [5] is performed with a substrate vertically immersed into the colloidal suspension, where it is left standing for some minutes. After the stick of the colloidal spheres onto the substrate, it is withdrawn at low speed. Thicker films are fabricated increasing the withdrawn speed and/or the number of dips. Infiltration and template removal may be the subsequent steps (Fig. **14**).

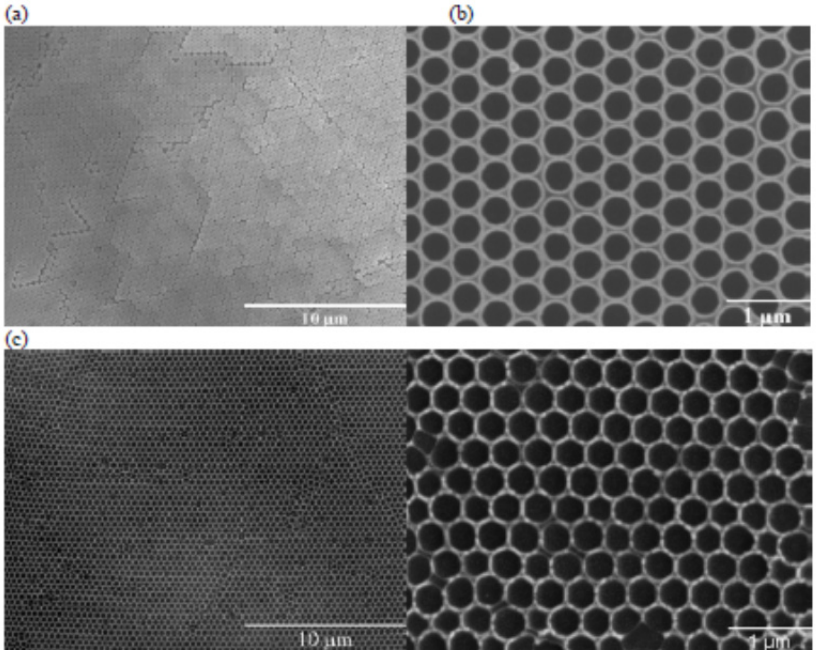

Figure 14: SEM images of artificial colloidal PC made from 460 nm self-assembled PS spheres, fabricated by dip-coating: (a) PS opal structure; (b) titania infiltrated PS template; (c) inverse opal (air spheres and titania matrix).

Sedimentation

Natural gem opals are obtained through sedimentation. To mimic this natural process, a sphere suspension is left to settle over a substrate, where sedimentation occurs, driven by gravity [35-37]. The sediment is then dried and heat treated. The final product is a compact of self-assembled spheres in a *fcc* and/or *hc* structures. For low colloidal concentrations (~1 wt%), the sphere size can be accurately determined from Stokes'law [36], if the density and viscosity are known.

Although the self-organization of the colloid results in a crystalline *fcc* or *hc* structure, the processing time may take a few days, up to several weeks.

Vertical Electric Field

A concentrated suspension of magnetic or superparamagnetic NPs is closed in a glass cell composed of two ITO glasses (brand indium-tin-oxide coated microscope glasses). The positive and negative poles of the DC power source are connected to the upper and bottom ITO glasses of the unit cell. It is possible to control magnetic field strength applied to the sample, by changing either the distance between the sample and the permanent magnet, or the current in electromagnets. The electric field strength is controlled by setting the output voltage of the DC power source. A responsive PC, which changes its reflection wavelength under external electric or electromagnetic stimulus, is produced (Fig. **15**) [61-62].

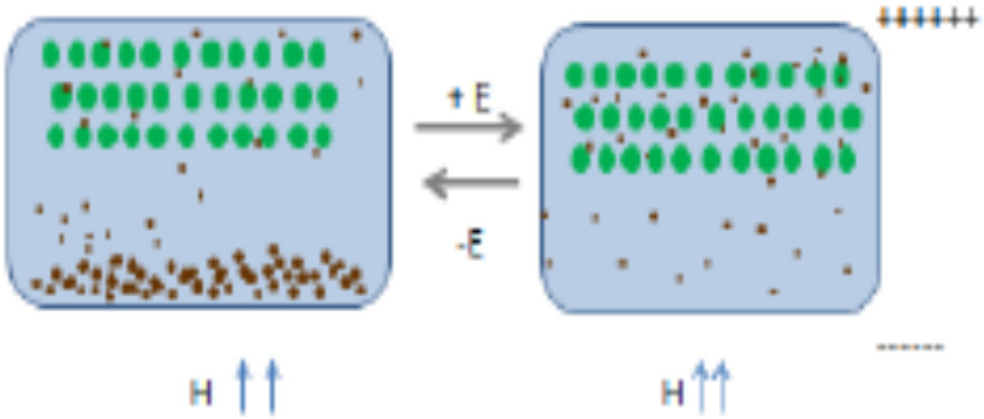

Figure 15: Migration and distribution of magnetic NPs in the presence of the electric field (adapted from [61]).

Langmuir-Blodgett Method

In Langmuir-Blodgett methodology a molecular monolayer is formed by spreading amphiphilic entities at the air-water interface. It develops by immersing a hydrophilic substrate into water, drawn it slowly upwards, while a monolayer of amphiphilic molecules stands by it, changing the surface to hydrophobic (Fig. **16**). By careful control the solvent evaporation, 2D opal structures may be obtain on a glass substrate, with the (111) growth axis of the fcc lattice normal to the substrate [63, 64].

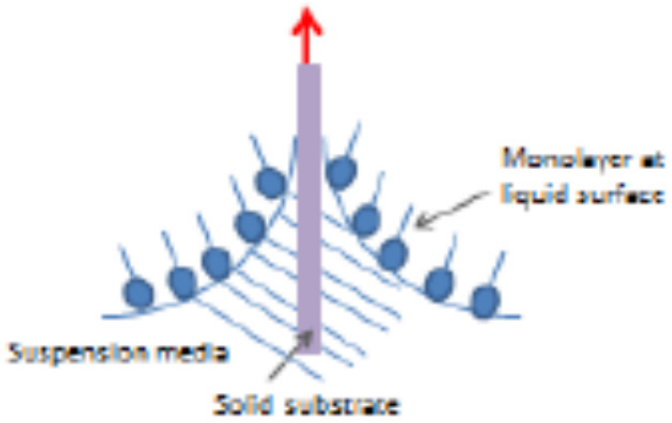

Figure 16: The Langmuir-Blodgett film formation.

Patterned Substrates

New promises come up when the substrate has been micro-patterned. Based on the wide range of soft lithography possibilities, a multitude of structures with different shapes and architectures can be fabricated.

Patterned substrates are a simple and very efficient way to template PC structures. SiNx-based PCs patterns were fabricated by a UV nanoimprint lithography process of the ITO electrode layer of a GaN-based light-emitting diode (LED) device on a patterned sapphire substrate (PSS). 19% increased in electroluminescence intensity was observed when compared with the unpatterned LED device, at 445 nm wavelength [65]. A 3D PC was produced by auto-cloning the PSS with alternate Ta2O5 and SiO2 coatings. A full band gap PC was

obtained at 410-470 nm wavelength range, matching the emission spectrum of the gallium nitride (GaN) light-emitting diode (LED) [66].

6. PHOTONIC CRYSTALS APPLICATIONS

As we have seen, PCs are attractive candidates to create optical materials and devices used to control and manipulate the flow of light [3]. PCs have inspired considerable enthusiasm because of their scientific and technological significance. For example, 1D PCs are in widespread use for thin-film optics in applications such as low and high reflection coatings on lenses and mirrors, or color changing paints and inks; even 1D PCs have been proposed for sensing applications [67]. Higher-dimensional PCs have proved to be of interest for both fundamental and applied research. 2D PC structures, as an example, are entering the market in applications such as fibers, taking advantage of a microscale structure to modulate light, for applications in nonlinear devices and guiding peculiar wavelengths. Moreover, 2D PCs have also been applied commercially to fabricate vertical cavity surface emitting lasers. 3D PCs attract considerable research interest because light can be modulated in all directions. With proper geometry and large enough refractive index contrast, a complete PBG may be present where light cannot propagate in any direction. This property facilitates various applications in devices such as optical switches, sensors, filters and waveguides [68, 69]. The 3D PCs, although far from entering the market, promise optical nonlinearity, needed for optical transistors used in optical computers.

More concretely, in the last several years, PCs have inspired a lot of engineering/commercial applications namely: localization of lightwave [70], inhibition of spontaneous emission [71, 72], lasers [73-75], waveguides [76-80], splitters [81-83], fibers [84], antennas [85, 86], optical circuits, resonant cavities and filters [3, 87, 88], time delay, dispersion control [1] and ultrafast optical switches [89]. PCs have been also proposed for sensing applications [90] and also photonic crystals have been proposed for the simultaneous control of both photonic and phononic waves, achieving novel alike control of light and sound in very small regions will be achieved, by merging both fields (nanophotonics and nanophononics) within a common platform [91].

6.1. Waveguiding Through Localized Coupled Cavities

As we have seen, PBG structures supply a promising instrument for the control of the flow of light in integrated optical devices. Hence, there has been an increasing interest in developing PC-based waveguide components capable of guiding and

bending EM waves either along a line defect [77], [80] or through coupled cavities [79]. Fig. **17** shows the first case, where light is confined in a direction perpendicular to the axis of the missing PBG elements, whilst photons are able to propagate in other directions parallel to the axis of the missing elements.

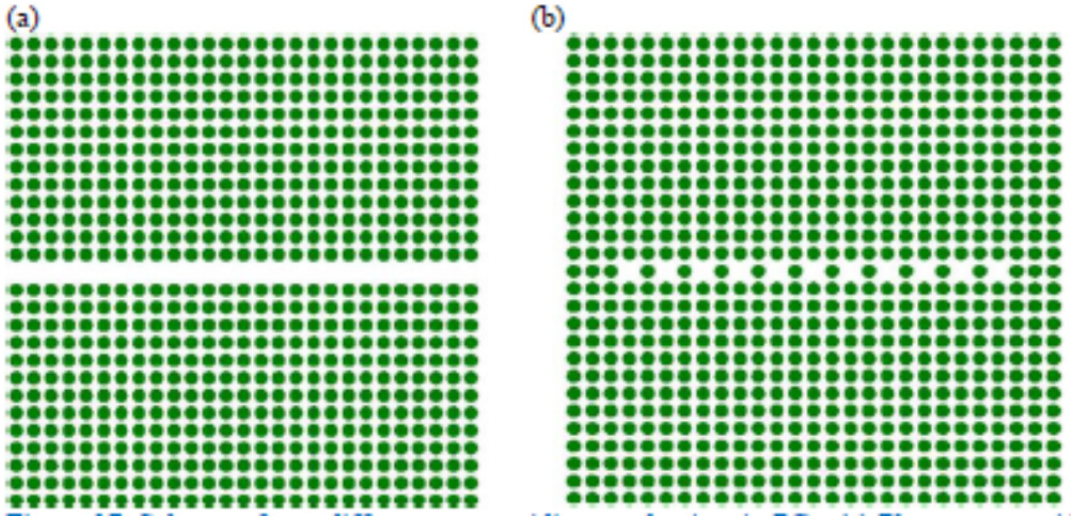

Figure 17: Scheme of two different waveguiding mechanisms in PCs. (a) Planar waveguides (PW) consist of two parallel PCs mirrors with a suitable gap between (the two of) them. (b) CCWs are formed introducing several defects (cavities) in 2D PCs.

In addition, in the second case, which it is known as coupled-cavity waveguides (CCW) [92], the EM waves are tightly restricted at each defect site, and photons are able to propagate thanks to interactions among the neighboring cavity modes [Fig. **17** (b)]. To explain this guiding effect, it is important to first understand what happens when a single defect is introduced in perfect PCs.

By removing from or adding materials to a PC, it is possible to generate localized EM modes inside the PBG which are analogues to the acceptor and donor impurity states in a semiconductor [93, 94]. Henceforth, photons with specific wavelengths can be locally trapped inside the defect volume (cavity).

Introducing several defects in the structure, as shown if Fig. **17**(b), a propagation mechanism for photons along localized coupled cavity modes in PCs was theoretically proposed [95-97,] and experimentally demonstrated [92]. This propagation effect could be explained by Tight-Binding theory, firstly used to understand the overlap of atomic wave functions in condensed-matter. Physics [92] and has also been successfully applied to photonic structures [92, 95]. In the

CCW structures (as shown in see Fig. **17** (b)), photons can hop from one tightly confined mode to the neighboring one due to weak interactions between them. The CCW structures have not only proposed for guiding and bending, but also for various applications based on coupled-cavities as splitting, switching, delay lines have been also proposed and demonstrated [95-98].

6.2. Waveguide Bends

The bending in standard waveguides, in photonic integrated circuits, presents two main drawbacks: first, light may be reflected and secondly, light may be radiated. This radiation effect increases when sharper bends are used and imposes restrictions for designers. For example in low-contrast technology based on silica, bend radii of several millimeters are required in order to minimize radiation losses [99], what supposes a big penalty in circuit integration. In high contrast technology, as for example silicon on insulator, the bend radii can be reduced (microns range) achieving small radiation losses.

The use of PC structures can improve the bending behavior in photonic integrated circuit since the structure inherent band gap prohibits radiation losses and designers have only to fight against reflection losses. Moreover, and as shown in ref. [3], it is possible to find PBG bend structures where the reflection loss is zero, achieving, at certain frequencies, a PC-based bend which exhibits a 100% transmission even when the bend radius is smaller than the wavelength. Fig. **18** shows the proposed in ref. [3] 100% transmission bend based on PCs.

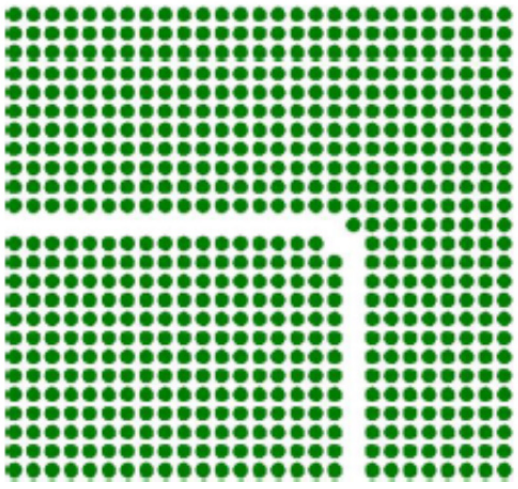

Figure 18: Scheme of a sharp 90º bend in a PC waveguide structure.

In ref. [3] the coupled mode theory was used to explain structures as those shown in Fig. **18**. We may imagine the bend corner as a weak (low-Q) cavity, coupled to two waveguides. By symmetry, the corner resonator must decay the same signal intensity in both horizontal and vertical directions (while no other radiation channels are observed). In that case and supposing that the structure is weakly coupled, the transmission peaks are 100% on resonance.

6.3. Sensors

In a sensor device, a tailored material is applied onto a physical transducer to convert a variation in one of its properties into a measurable physical signal. Sensors must own specific characteristics, particularly: sensitivity, dynamic range, accuracy, absence of hysteresis and linearity, high signal to noise ratio, resolution and bandwidth [100, 101]. Numerous PC-based sensors have been developed with the goal of physical [102-109], chemical [102, 110-115] and biological [116-121] parameter sensing. As an example, a strain-sensor is illustrated on Fig. **19** [122]. Here an opal has been deposited over a flexible substrate. The material deformation under an applied stress (or strain) [102, 109] causes a mechano-optical effect [105, 108, 123]. In the present example, the substrate was a chemical resistant, polyimide tape, as a result of its stable physical and mechanical properties over a wide temperature range, very low creep and high tensile strength [124, 125].

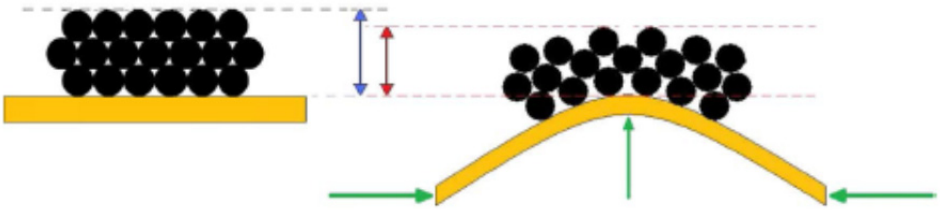

Figure 19: Opal deposited over a flexible substrate: flat (left) and bent (right). Bending stress results in an elastic deformation of the material, between flat (0º, without bending) and bent (45º off flat) positions [122].

CONCLUSIONS

PCs materials have been demonstrating their potential, are currently a mainstream concept and certainly become an imperative player in the near future. PCs have been addressed from many scientific and technological top-down and bottom-up techniques. Among them, self-assembly (a bottom-up approach) has probably bringing about more scientific aspects due to the fact that they are suitable to be

manufactured by a large diversity of methods, on very large variety of materials and numerous objectives.

ACKNOWLEDGEMENTS

Declared None.

CONFLICT OF INTEREST

The authors confirm that this chapter contents have no conflict of interest.

REFERENCES

[1] Hinton HE, Gibbs DF. J. An electron microscope study of the diffraction gratings of some carabid beetles Insect Physiol 1969; 15: 959-960.
[2] Sanders JV. Colour of Precious Opal. Nature 1964; 204: 1151-1153.
[3] Joannopoulos JD, Johnson SG, Meade RD, Winn JN. Photonic Crystals Molding the flow of light. Princeton University Press 2008; 305.
[4] Almeida RM, Wang Z. Sol-gel preparation of one-dimensional photonic bandgap structures. In: Adibi A, Scherer A, Lin S-Y, Eds. Photonic Bandgap Materials and Devices. Proceedings SPIE 2002; 2002 April 24-26, San Jose, CA, USA; 24-33.
[5] Almeida RM, Portal S. Photonic band gap structures by sol-gel processing. Curr Opin Solid State Mater Sci 2003; 7: 151-157.
[6] Almeida RM, Rodrigues AS. Photonic bandgap materials and structures by sol–gel processing. J Non-Cryst Solids 2003; 326-327: 405-409.
[7] Almeida RM, Gonçalves MC, Portal S. 3-D rare earth-doped colloidal photonic crystals. J Non-Cryst Solids 2004; 345&346: 562-569.
[8] Almeida RM, Gonçalves MC. Sol-Gel derived photonic bandgap structures. In: Balda R, Eds. Pandalai SG, Managing Eds. Photonic Glasses. Ontario, Canada: Research Signpost 2006; pp.1-22. (ISBN 81-308-0063-2)
[9] Almeida RM, Gonçalves MC. Crystallization of sol-gel derived glasses, I J Applied Glass Science 2014; 5(2): 114-125.
[10] Soukoulis CM, Eds. Photonic Crystals and Light Localization in the 21st Century. Kluwer Academic Publishers: Dordrecht, the Netherlands 2001.
[11] Johnson SG, Joannopoulos JD. Introduction to photonic crystals. MIT (US) 16 (2003).
[12] Mach P, Wiltzius P, Megens M, et al. Electro-optic response and switchable Bragg diffraction for liquid crystals in colloid-templated materials. Phys Rev E 2002; 65: 031720-1 – 031720-3.
[13] Koenderink AF, Bechger L, Schriemer HP, Lagendijk A, Vos WL. Broadband fivefold reduction of vacuum fluctuations probed by dyes in photonic crystals. Phys Rev Lett 2002; 88(143903): 1-4.
[14] López C. Materials Aspects of Photonic Crystals. Adv Mater 2003; 15: 1679–1704.
[15] Anselmann R, Winkler H. Ordered Structures from Nanoparticles. Adv Eng Materials 2003; 5(8): 560-562.
[16] Lopez C, Vazquez L, Meseguer F, Mayoral R, Ocana M, Miguez H. Photonic crystal made by close packing SiO2 submicron spheres. Superlattices Microstruct 1997; 22: 399-404.
[17] King JS, Heineman D, Graugnard E, Summers CJ. Atomic layer deposition in porous materials: 3D photonic crystals. Appl Surf Science 2005; 511-516.
[18] Ding L, Belacel C, Ducci S, Leo G, Favero I. Ultralow loss single-mode silica tapers manufactured by a microheater. Appl Opt 2010; 49: 2441-2445.
[19] Santamaria FG, Miyazaki HT, Urquia A, et al. Nanorobotic Manipulation of Microspheres for On-Chip Diamond Architectures. Adv Mater 2002; 14(8): 1144-1147.

[20] Noda S, Tomoda K, Yamamoto N, Chutinan A. Full three-dimensional photonic bandgap crystals at near-infrared wavelengths, Science 2000; 289: 604-606.
[21] Lin SY, Chow E, Hietala V, Villeneuve PR, Joannopoulos JD. Experimental demonstration of guiding and bending of electromagnetic waves of photonic crystal. Science 1998; 282: 274-276.
[22] Zavieh L, Mayer TS. Demonstration of a three-dimensional simple-cubic infrared photonic crystal. Appl Phys Lett 1999; 75: 2533-2535.
[23] Divliansky I, Mayer TS, Holliday KS, Crespi VH. Fabrication of three-dimensional polymer photonic crystal structures using single diffraction element interference lithography. Appl Phys Lett 2003; 82: 1667-1669.
[24] Campbell M, Sharp DN, Harrison MT, Denning RG, Turberfield AJ. Fabrication of photonic crystals for the visible spectrum by holographic lithography. Nature 2000; 404: 53-56.
[25] Sun HB, Matsuo S, Misawa H. Three-dimensional photonic crystal structures achieved with two-photon-absorption photopolymerization of resin. Appl Phys Lett 1999; 74: 786-788.
[26] Yang S, Megens M, Aizenberg J, Wiltzius P, Chaikin PM, Russel WB. Creating periodic threedimensional structures by multibeam interference of visible laser. Mater Chem 2002; 14: 2831-2833.
[27] Wang X, Xu JF, Su HM, et al. Appl. Phys. Lett. Three-dimensional photonic crystals fabricated by visible light holographic lithography. Appl Phys Lett 2003; 82(14): 2212-2214.
[28] Shoji S, Kawata S. Photo-fabrication of three-dimensional photonic crystal by multi-beam laser interference into a photopolymerizable resin. Appl Phys Lett 2000; 76: 2668-2670.
[29] Kamenetzky EA, Mangliocco LG, Panzer HP, Structure of solidified colloidal array laser filters studied by cryogenic transmission electron microscopy. Science 1994; 263: 207-210.
[30] Clark NA, Hurd AJ, Ackerson BJ. Single colloidal crystals. Nature 1979; 281: 57-60.
[31] Sunkara HB, Jethmalani JM, Ford WT. Composite of colloidal crystals of silica in poly(methyl methacrylate). Chem Mater 1994; 6: 362-364.
[32] Weissman M, Sunkara HB, Tse AS, Asher SA. Thermally Switchable Periodicities from Novel Mesocopically Ordered Materials. Science 1996; 274: 959-960.
[33] Cheng Z, Russel WB, Chalkin PM. Controlled growth of hard-sphere colloidal crystals. Nature 1999; 401: 893-895.
[34] Miguez H, Lopez C, Meseguer F, et al. Photonic crystal properties of packed submicrometric SiO_2 spheres. Appl Phys Lett 1997; 71: 1148-1150.
[35] Pusey PN, van Megen W. Phase behaviour of concentrated suspensions of nearly hard colloidal spheres. Nature 1986; 320: 340-342.
[36] Miguez H, Messeguer F, Lopez C, et al. Control of the photonic crystal properties of fcc-packed submicrometer SiO_2 spheres by sintering. Adv Mater 1997; 10: 480-483.
[37] Miguez H, Meseguer F, Lopez C, Mifsud A, Moya JS, Vazquez L. Evidence of fcc crystallization of SiO_2 nanospheres. Langmuir 1997; 13(23): 6009-6011.
[38] Trau M, Saville DA, Aksay IA. Field Induced Layering of Colloidal Crystals. Science 1996; 272: 706-709.
[39] Hayward RC, Saville DA, Aksay IA. Electrophoretic assembly of colloidal crystals with optically tunable micropatterns. Nature 2000; 404(6773): 56-59.
[40] Holgado M, Garcia-Santamaria F, Blanco A, et al. Electrophoretic deposition to control artificial opal growth. Langmuir 1999; 15: 4701-4704.
[41] Wen W, Wang N, Ma H, Lin Z, Tam WY, Chan CT, Sheng P. Field Induced Structural Transition in Mesocrystallites. Phys Rev Lett 1999; 82: 4248-4251.
[42] van Blaaderen A, de la Rue R, Wiltzius P. Template-directed colloidal crystallization. Nature 1997; 385: 321-324.
[43] Xia Y, Gates B, Yin Y, Lu Y. Monodispersed Colloidal Spheres: Old Materials with New Applications. Adv Mater 2000; 12: 693-713.
[44] Park SH, Qin D, Xia Y. Crystallyzation of mesoscale particles over large areas. Adv Mater 1998; 10: 1028-1032.
[45] Mei D, Liu H, Cheng B, Li Z, Zhang D, Dong P. Visible and near-infrared silica colloidal crystals and photonic gaps. Phys Rev B 1998; 58: 35.
[46] Blanco A, Chomski E, Grabtchak S, et al Large-scale synthesis of a silicon photonic crystal with a complete three-dimensional bandgap near 1.5 micrometres. Nature 2000; 405(6785): 437-440.

[47] Jiang P, Bertone JF, Hwang KS, Colvin VL. Single-Crystal Colloidal Multilayers of Controlled Thickness. Chem Mater 1999; 11: 2132-2140.
[48] Dimitrov AS, Dushkin CD, Yosimura H, Nagayama K. Observations of lattex particle two dimensional-crystal nucleation in wetting films on mercury, glass and mica. Langmuir 1994; 10: 432-440.
[49] Denkov ND, Velev OD, Kralchevsky PA, Ivanov IB, Yoshimura H, Nagayama K. Twodimensional crystallization. Nature 1999; 361: 26-26.
[50] Gu ZZ, Fujishima A, Sato O. Fabrication of High-Quality Opal Films with Controllable Thickness. Chem Mater 2002; 14: 760-765.
[51] Vlasov YA, Bo XZ, Sturm JC, Norris DJ. On-chip *natural* assembly of silicon photonic bandgap crystals. Nature 2001; 414(6861): 289-293.
[52] Kozhukharov V, Trapalis C, Samuneva B, Kirilova E. J. Sol-gel processing of multilayer thin coatings. Mater Sci Lett 1992; 11: 1206-1208.
[53] Trapalis CC, Karakassides MA, Kordas G, Aslanoglou X. Study of a multilayer wavelenght selective reflector prepared by the sol-gel process. Mater Lett 1995; 25: 265-269.
[54] Belessa J, Rabaste S, Plenet JC, Dumas J, Mugnier J, Marty O. Eu^{3+} -doped microcavities fabricated by sol–gel process. Appl Phys Lett 2001; 79: 2142-2144.
[55] Rabaste S, Bellessa J, Brioude A, et al. Thin Solid Films 2002; 416: 242-247.
[56] Biswas PK, Kundu D, Ganguli D. J. Preparation of wavelength-selective reflector by sol-gel processing. Mater Sci Lett 1987; 6: 1481-1482.
[57] Kundu D, Biswas PK, Ganguli D. Sol-gel preparation of wavelength-selective reflecting coatings in the system ZrO_2-SiO_2. J Non-Cryst Solids 1989; 110: 13-16.
[58] Chen KM, Sparks AW, Luan H-C, Lim DR, Wada K, Kimerling LC. SiO_2/TiO_2 omnidirectional reflector and microcavity resonator via sol gel method. Appl Phys Lett 1999; 75: 3805-3809.
[59] Zhang Q, Li X, Shen J, Wu G, Wang J, Chen L. ZrO_2 thin films and ZrO_2/SiO_2 optical reflection filters deposited by sol-gel method. Mater Lett 2000; 45: 311-314.
[60] Miguez H, Blanco A, Lopez C, et al. Face centered cubic photonic bandgap materials based on opal-semiconductor composites. J Lightwave Technol 1999; 17: 1975-1981.
[61] Liu J, Mao Y, Ge J. J. Materials Chemistry C 2013; 1: 6129.
[62] Ge J, He L, Goebl J, Yin Y. Assembly of Magnetically Tunable Photonic Crystals in Nonpolar Solvents. J Am Chem Soc 2009; 131: 3484-3486.
[63] Romanov SG, Bardosova M, Povey IM, Pemble ME, Sotomayor Torres CM. Understanding of transmission in the range of high-order photonic bands in thin opal film. Appl Physics Letters 2008; 92: 191106-191106-3
[64] Bardosova M, Pemble ME, Povey IM, Tredgold RH. The Langmuir-Blodgett approach to making colloidal photonic crystals from silica spheres. Adv Mater 2010; 22: 3104-3124.
[65] Byeon KJ, Cho JY, Kim J, Park H, Lee H. Fabrication of SiNx-based photonic crystals on GaN-based LED devices with patterned sapphire substrate by nanoimprint lithography. Opt Express 2012; 20(10): 11423-32.
[66] Ku HM, Huang CY, Chao S. Fabrication of three-dimensional autocloned photonic crystal on sapphire substrate. Appl Opt 2011; 50(9): C1-4.
[67] Francisco J, Aparicio et al., Transparent Nanometric Organic Luminescent Films as UV-Active Components in Photonic Structures. Advanced Materials 2011; 23 (6): 761-765.
[68] Jang JH, Ullal CK, Maldovan M, et al. 3D micro-and nanostructures via interference lithography. Advanced Functional Materials 2007; 17: 3027-3041.
[69] Moon JH, Ford J, Yang S. Fabricating three-dimensional polymeric photonic structures by multi-beam interference lithography. Polymers for Advanced Technologies 2006; 17: 83-93.
[70] John S. Strong localization of photons in certain disordered dielectric superlattices. Phys Rev Lett 1987; 58: 2486–2489.
[71] Yablonovitch E. Inhibited spontaneous emission in solid-state physics and electronics. Phys Rev Lett 1987; 58: 2059–2062.
[72] Boroditsky M, Vrijen R, Krauss TF, Coccioli R, Bhat R, Yablonovitch E. Spontaneous emission extraction and Purcell enhancement from thin-film 2-D photonic crystals. J Lightwave Technol 1999; 17: 2096–2112.
[73] Painter O, Lee RK, Scherer A, et al. Two-dimensional photonic band-gap defect mode laser. Science 1999; 284: 1819–1821.

[74] Mekis A, Meier M, Dodabalapur A, Slusher RE, Joannopoulos JD. Lasing mechanism in two-dimensional photonic crystallasers. Appl Phys A: Materials Science & Processing 1999; 69: 111–114.
[75] Noda S, Yokoyama M, Imada M, Chutinan A, Mochizuki M. Polarization mode control of two-dimensional photonic crystal laser by unit cell structure design. Science 2001; 293: 1123–1125.
[76] Mekis A, Chen JC, Kurland I, Fan S, Villeneuve PR, Joannapoulos JD. High transmission through sharp bends in photonic crystal waveguides. Phys Rev Lett 1996; 77: 3787–3790.
[77] Lin SY, Chow E, Hietala V, Villeneuve PR, Joannopoulos JD. Experimental demonstration of guiding and bending of electromagnetic waves in a photonic crystal. Science 1998; 282: 274–276.
[78] Temelkuran B, Ozbay E. Experimental demonstration of photonic crystal based waveguides. Appl Phys Lett 1999; 74: 486–488.
[79] Bayindir M, Temelkuran B, Ozbay E. Propagation of photons by hopping: A waveguiding mechanism through localized coupled-cavities in three-dimensional photonic crystals. Phys Rev B 2000; 61: R11855–11858.
[80] Loncar M, Nedeljkovic D, Doll T, Vuckovic J, Scherer A, Pearsall TP. Waveguiding in planar photonic crystals. Appl Phys Lett 2000; 77: 1937–1939.
[81] Yonekura J, Ikeda M, Baba T. Analysis of finite 2-d photonic crystals of columns and lightwave devices using the scattering matrix method. J Lightwave Technol 1999; 17: 1500–1508.
[82] Ziolkowski RW, Tanaka M. FDTD analysis of PBG waveguides, power splitters and switches. Opt Quant Electron 1999; 31: 843–855.
[83] Sondergaard T, Dridi KH. Energy flowin photonic crystalwaveguides. Phys Rev B 2000; 61: 15688–15696.
[84] Knight JC, Broeng J, Birks TA, Russell PJ. Photonic band gap guidance in optical fibers. Science 1998; 282: 1476–1479.
[85] Brown ER, Parker CD, Yablonovitch E. Radiation properties of a planar antenna on a photonic-crystal substrate. J Opt Soc Amer B 1993; 10; 404–407.
[86] Temelkuran B, Bayindir M, Ozbay E, et al. Photonic crystal based resonant antenna with a very high directivity. J Appl Phys 2000; 87: 603–605.
[87] Kosaka H, Kawashima T, Tomita A, et al. Photonic crystals for micro lightwave circuits using wavelength-dependent angular beam steering. Appl Phys Lett 1999; 74: 1370–1372.
[88] Lustrac A, Gadot F, Cabaret S, et al. Experimental demonstration of electrically controllable photonic crystals at centimeter wavelengths. Appl Phys Lett 1999; 75: 1625–1627.
[89] Villeneuve PR, Abrams DS, Fan S, Joannopoulos JD. Single-mode waveguide microcavity for fast optical switching. Opt Lett 1996; 21: 2017–2019.
[90] García-Rupérez J., et. al. Label-free antibody detection using band edge fringes in SOI planar photonic crystal waveguides in the slow-light regime. Optics Express 2010; 18(23): 24276-24286.
[91] Gomis-Bresco J, Navarro-Urrios D, Oudich M. et al. A one-dimensional optomechanical crystal with a complete phononic band gap. Nature Communications 2014; 5, 4452.
[92] Bayindir M, Temelkuran B, Ozbay E. Tight-binding description of the coupled defect modes in three-dimensional photonic crystals. Physical Rev Lett 2000; 84: 2140–2143.
[93] Yablonovitch E, Gmitter TJ, Meade RD, Rappe AM, Brommer KD, Joannopoulos JD. Donor and acceptor modes in photonic band structure. Phys Rev Lett 1991; 67: 3380–3383.
[94] Ozbay E, Tuttle G, Sigalas MM, Soukoulis CM, Ho KM. Defect structures in a layer-by-layer photonic band-gap crystal. Phys Rev B 1995; 51: 13961–13965.
[95] Ozbay E, Bayindir M, Bulu I, Cubukcu E. Investigation of Localized Coupled-Cavity Modes in Two-Dimensional Photonic Bandgap Structures. IEEE Jounal of Quantum Electronics 2002; 38(7): 837-843.
[96] Bayindir M, Temelkuran B, Ozbay E. Photonic crystal based beam splitters. Appl Phys Lett 2000; 77: 3902–3904.
[97] Lan S, Nishikawa S, Wada O. Leveraging deep photonic band gaps in photonic crystal impurity bands. Appl Phys Lett 2001; 78: 2101–2103.
[98] Lan S, Nishikawa S, Ishikawa H, Wada O. Design of impurity band-based photonic crystal waveguides and delay lines for ultrashort optical pulses. J Appl Phys 2001; 90: 4321–4327.
[99].Li YP, Henry CH. Silica-based optical integrated circuits. In: IEE. Proceedings on Optoelectronics; 1996 Oct; 143(5) pp. 263-280.
[100] Wilson JS, Eds. Sensor Technology Handbook. Elsevier: Amsterdam, Boston, 2005.

[101] Potyrailo RA, Mirsky VM. Combinatorial and high-throughput development of sensing materials: the first 10 years. Chemical Reviews 2008; 108: 770-813.
[102] Fudouzi H, Optical properties caused by periodical array structure with colloidal particles and their applications. Advanced Powder Technology 2009; 20(5): 502-508.
[103] Pursiainen OLJ, Baumberg JJ, Ryan K, et al. Compact strain-sensitive flexible photonic crystals for sensors. Appl Phys Letters 2005; 87.
[104] Pursiainen OLJ, Baumberg JJ, Winkler H, Viel B, Spahn P, Ruhl T. Shear-Induced Organization in Flexible Polymer Opals. Advanced Mater 2008; 20: 1484-1487.
[105] Wohlleben W, Bartels FW, Altmann S, Leyrer RJ. Mechano-optical octave-tunable elastic colloidal crystals made from core-shell polymer beads with self-assembly techniques Langmuir 2007; 23: 2961-2969.
[106] Li J, Wu Y, Fu J, Cong Y, Peng J, Han YC. Reversibly strain, tunable elastomeric photonic crystals. Chem Phys Letters 2004; 390: 285-289.
[107] Kim S, Gopalan V, Strain-tunable photonic band gap crystals. Appl Phys Letters 2001; 78: 3015-3017.
[108] Chiappini A, Armellini C, Battisti L, et al. Mechanochromic photonic crystals as strain sensors. In: MEMS, MOEMS, ICs and Electronic Components. Proceedings of Smart System Integration, European Conference & Exhibition on Integration Issues of Miniaturized Systems; 2010 March 23-24; Como, Italy.
[109] Zonta D, Chiappini A, Chiasera A, et al. in: Tomizuka M, Eds. Photonic Crystals for Monitoring Fatigue Phenomena in Steel Structures. Proceedings of SPIE; 2009 march 9-12; San Diego, CA, US 2009; pp. 23–4.
[110] Xia YN, Gates B, Yin YD, Lu Y. Monodispersed colloidal spheres. Old materials with new applications. Adv Materials 2000; 12: 693-713.
[111] Tian ET, Wang JX, Zheng YM, Song YL, Jiang L, Zhu DB. J. Mater Chem 2008; 18(10): 1116-1122.
[112] Holtz JH, Asher SA. Polymerized colloidal crystal hydrogel films as intelligent chemical sensing materials. Nature 1997; 389: 829-832.
[113] Sutti A, Baratto C, Calestani G, et al. Inverse opal gas sensors: Zn(II)-doped tin dioxide systems for low temperature detection of pollutant gases. Sensors and Actuators B: Chemical 2008; 130(1): 567-573.
[114] Arsenault AC, Kitaev V, Manners I, Ozin GA, Mihi A, Miguez H. Vapor swellable colloidal photonic crystals with pressure tunability. J Mater Chem 2005; 15(1): 133-138.
[115] Scott RWJ, Yang SM, Chabanis G, Coombs N, Williams DE, Ozin GA. Tin Dioxide Opals and inverted Oplas: Near-Ideal Microstrutures for Gas Sensors. Adv Mater 2001; 13(19): 1468-1472.
[116] Fleischhaker F, Lange B, Zentel R. Functional Opals from Reactive Polymers: Complex Structures, Sensors, and Modified Photoluminescence. In: Adler H-J, Kuckling D, Eds. Reactive Polymers in Inhomogeneous Systems, in Melts, and at Interfaces. Proceedings of Macromolecular Symposia; 2007 August; Verlag GmbH & Co. KGaA, Weinheim 254(1) pp. 210-216.
[117] Sharma AC, Jana T, Kesavamoorthy R, et al. A General Photonic Crystal Sensing Motif: Creatinine in Bodily Fluids. J Amer Chem Society 2004; 126: 2971-2977.
[118] Nakayama D, Takeoka Y, Watanabe M, Kataoka K. Simple and precise preparation of a porous gel for a colorimetric glucose sensor by a templating technique. Angewandte Chemie International Edition 2003; 42(35): 4197-4200.
[119] Asher SA, Alexeev VL, Goponenko AV, et al. *Photonic crystal carbohydrate sensors: low ionic strength sugar sensing* J Am Chem Soc 2003; 125: 3322-3329.
[120] Qian WP, Gu ZZ, Fujishima A, Sato O. Three-dimensionally ordered macroporous polymer materials: An approach for biosensor applications. Langmuir 2002; *18*(11): 4526-4529.
[121] Griol A, Climentb E, Ortuñoc R, et al. Dual sensor based on molecular gates and plasmonic structures (extended abstract). In: Proceedings 40th Micro and Nano Engineering; 2014 Sept 22-26; Lausanne, Switzerland.
[122] Fortes LM, Gonçalves M, Almeida RM. Flexible Photonic Crystals for Strain Sensing, Opt Materials 2011; 33: 408-412.
[123] Ozin GA, Arsenault AC. P-Ink and Elast-Ink from lab to market. Materials Today 2008; 11: 44-51.
[124] Hay GI, Evans PSA, Harrison DJ, Southee D, Simpson G, Harrey PM. Conductive lithographic film fabricated resistive strain gauges. In: Proceedings of the IEEE Sensors 2003 1 and 2; 2003 Oct 22-24; pp. 248-252.
[125] Han JS, Tan ZY, Sato K, Shikida M. Thermal characterization of micro heater arrays on a polyimide film substrate for fingerprint sensing applications. J Micromechanics and Microengineering 2005; 15: 282-289.